ACS Catalysis

pubs.acs.org/acscatalysis

Research Article

Metal–Support Interactions and C1 Chemistry: Transforming Pt-CeO_2 into a Highly Active and Stable Catalyst for the Conversion of Carbon Dioxide and Methane

Feng Zhang, Ramón A. Gutiérrez, Pablo G. Lustemberg, Zongyuan Liu, Ning Rui, Tianpin Wu, Pedro J. Ramírez, Wenqian Xu, Hicham Idriss, M. Verónica Ganduglia-Pirovano,* Sanjaya D. Senanayake,* and José A. Rodriguez*

Cite This: *ACS Catal.* 2021, 11, 1613–1623

Read Online

ACCESS | Metrics & More | Article Recommendations | Supporting Information

ABSTRACT: There is an ongoing search for materials which can accomplish the activation of two dangerous greenhouse gases like carbon dioxide and methane. In the area of C1 chemistry, the reaction between CO_2 and CH_4 to produce syngas (CO/H_2), known as methane dry reforming (MDR), is attracting a lot of interest due to its green nature. On Pt(111), high temperatures must be used to activate the reactants, leading to a substantial deposition of carbon which makes this metal surface useless for the MDR process. In this study, we show that strong metal–support interactions present in Pt/CeO_2(111) and Pt/CeO_2 powders lead to systems which can bind CO_2 and CH_4 well at room temperature and are excellent and stable catalysts for the MDR process at moderate temperature (500 °C). The behavior of these systems was studied using a combination of in situ/*operando* methods (AP-XPS, XRD, and XAFS) which pointed to an active Pt-CeO_{2-x} interface. In this interface, the oxide is far from being a passive spectator. It modifies the chemical properties of Pt, facilitating improved methane dissociation, and is directly involved in the adsorption and dissociation of CO_2 making the MDR catalytic cycle possible. A comparison of the benefits gained by the use of an effective metal-oxide interface and those obtained by plain bimetallic bonding indicates that the former is much more important when optimizing the C1 chemistry associated with CO_2 and CH_4 conversion. The presence of elements with a different chemical nature at the metal-oxide interface opens the possibility for truly cooperative interactions in the activation of C–O and C–H bonds.

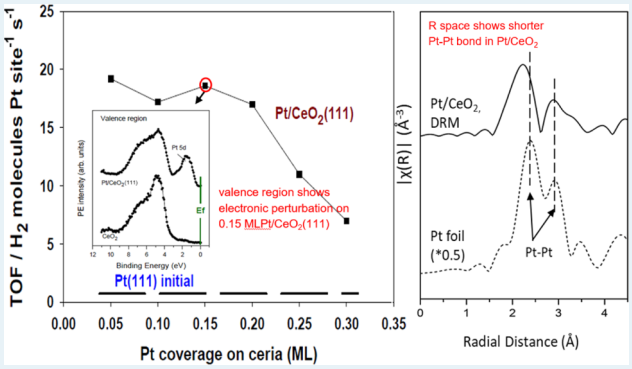

KEYWORDS: *C1 chemistry, CO_2 conversion, CH_4 conversion, methane dry reforming, platinum, metal–support interactions*

INTRODUCTION

Carbon dioxide (CO_2) is a common greenhouse gas emitted whenever coal, oil, or other carbon-rich fuels are burned. It is the largest contributor to climate change.[1] The conversion of CO_2 to high value chemicals or fuels is an important topic which is attracting a lot of attention worldwide. In nature, the methane molecule (CH_4) is highly abundant, being the simplest and most stable alkane compound. While methane does not linger as long in the atmosphere as carbon dioxide, it is far more devastating to the climate because of how effectively it absorbs heat.[3−5] CH_4 has a greenhouse warming potential (GWP) which is 84 times greater than that of CO_2. It has been estimated that methane can be responsible for 25% of already observed changes to Earth's climate.[3−5] CH_4 is the main component of natural gas and is frequently flared or vented into the atmosphere during oil and gas drilling operations. As in the case of CO_2, there are important environmental and commercial interests to activate and transform CH_4 into value-added chemicals (olefins, aromatics, and alcohols).[2,4,5]

In the area of C1 chemistry, the reaction between CO_2 and CH_4 to produce syngas (CO/H_2), methane dry reforming (MDR), has attracted a lot of interest due to its green nature.[6] The syngas produced by this reaction can be used in fuel cells fed with H_2, in the synthesis of methanol or other oxygenates, and in the production of hydrocarbons through the Fischer-Tropsch process.[6] Two main reactions in the MDR process involve the conversion of CO_2:

Received: October 28, 2020
Revised: December 22, 2020
Published: January 20, 2021

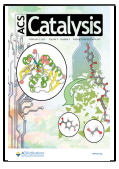

https://dx.doi.org/10.1021/acscatal.0c04694
ACS Catal. 2021, 11, 1613–1623

$$CO_2 + CH_4 \rightarrow 2CO + 2H_2 \ (\Delta H_{298K} = 247\ kJmol^{-1}) \quad (1)$$

$$CO_2 + H_2 \rightarrow CO + H_2O \ (\Delta H_{298K} = 41\ kJmol^{-1}) \quad (2)$$

In the second reaction, the reverse water-gas shift (RWGS), is often seen at high temperature. The MDR process is a real challenge due to the high stability and the nonpolar nature of both CO_2 and CH_4.[2,7−9] Heterogeneous catalysts are frequently used to accomplish this task and the activation of C−O and C−H bonds must be done in a concerted manner to avoid carbon deposition and subsequent deactivation of the catalyst.[6,8] When dealing with the activation of CO_2 and CH_4 on metal and oxide surfaces, a set of scaling relations and descriptors have been evaluated for the controlled cleavage of the C−O or C−H bonds in these molecules.[7−15] However, what types of systems can simultaneously activate CO_2 and CH_4? It has become clear that single metals alone are not efficient for the MDR process[16,17] and better results can be obtained when one uses metal−metal or metal-oxide interfaces where different sites cooperate in the activation of CO_2 and CH_4.[8,18−20]

In recent years, great research efforts have been made in order to develop metal/oxide catalysts with good activity, selectivity, and stability for the MDR process.[6,8] Systems which contain noble metals (Rh, Ru, Pt, and Ir) have received substantial attention since they can be very active and less sensitive to deactivation by carbon deposition than catalysts based on Ni or Co.[6,21−24] Pt and Pt alloys have been investigated showing a remarkable potential,[6,25−29] but important issues such as the effect of the metal particle size or morphology and the role of the support (Al_2O_3, MgO, CeO_2, ZrO_2, CeO_2-ZrO_2, and carbon) need to be addressed for optimizing this type of MDR catalysts.[6] In this article, we investigate the MDR process on well-defined Pt/CeO_2(111) and powder Pt/CeO_2 catalysts using a multitechnique approach.

On surfaces of noble metals, methane exhibits a rather low probability for dissociation which makes the effective conversion of the molecule difficult.[30−32] For example, in the case of clean Pt(111), used as a typical benchmark substrate in fundamental studies of hydrocarbon activation, a value of $\sim 1 \times 10^{-8}$ has been measured for the methane C−H dissociation probability at 25 °C.[32] At this temperature, the hydrocarbon molecule dissociates depositing C and CH_3 groups on the platinum surface. In the range of 100−200 °C, the formation of C−C bonds occurs yielding species such as ethylidyne (C_2H_3) and ethynyl (C_2H) on the platinum surface.[32] A carbonaceous layer eventually deactivates the chemical and catalytic properties of Pt(111).[32] The same occurs when Pt(100) or Pt(110)-(1×2) are exposed to methane at elevated temperature.[33,34] The platinum surfaces also show very poor activation of CO_2.[7] Neither Pt(111) nor Pt(100) bind carbon dioxide well.[7] Recent works have found special electronic and chemical properties in Pt atoms directly bonded to ceria,[35−37] but no systematic research has been carried out for the reaction of CO_2 and CH_4 over Pt-CeO_2 interfaces. Can metal−support interactions be useful for MDR and in the control of carbon deposition on platinum? In this article, we show clear evidence of metal−support interactions in the Pt/CeO_2 system and their effects in shifting the system away from the normal behavior of bulk Pt, producing active and stable catalysts for CO_2 and CH_4 activation in dry reforming.

RESULTS AND DISCUSSION

Reaction of CH_4 and CO_2 on Pt/CeO_2(111) Surfaces. We started by investigating the interaction of CH_4, CO_2, and CH_4/CO_2 mixtures with Pt/CeO_2(111) surfaces. Figure 1 shows valence photoemission spectra for a clean CeO_2(111) surface and a surface containing 0.15 monolayer(ML) of platinum. The valence spectrum for the ceria system exhibits the O 2p band between 8 and 3.5 eV with a large band gap below the Fermi level (E_f). The addition of Pt led to the appearance of new features centered at a binding energy of 2 to 1 eV. These features come from Pt 5d, 6s states. It is important to notice that the density of states (DOS) around the Fermi level for Pt/CeO_2(111) is close to zero. This is very different from the valence photoemission spectrum of bulk platinum, Pt(111) or Pt(100), where a very large DOS is seen at the Fermi level.[37−39] Thus, the Pt atoms in contact with ceria exhibit very strong electronic perturbations which can affect their chemical and catalytic properties. This phenomenon was seen over a wide range of temperatures (25−600 °C) but only at small coverages of Pt (< 0.2 ML). For higher coverages of the admetal (> 0.5 ML), the valence spectrum of Pt/CeO_2(111) eventually converged to that of bulk platinum and the novel chemical behavior of the admetal disappeared.[37] The data of photoelectron spectroscopy at low Pt coverages are consistent with previous theoretical studies which show electronic perturbations when atoms or small clusters of the metal are in contact with a ceria surface.[33−35,40,41]

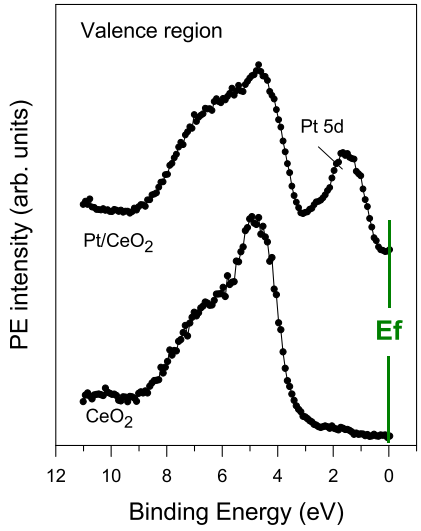

Figure 1. He-II valence photoelectron spectra collected before and after deposition of 0.15 ML of Pt on a CeO_2(111) surface.

Figure 2 displays C 1s X-ray photoelectron spectroscopy (XPS) spectra recorded after dosing CH_4 at 25 °C to plain CeO_2(111) and surfaces precovered with 0.15 and 0.25 ML of platinum. CeO_2(111) did not dissociate the alkane molecule at 25 °C. In contrast, methane dissociation occurred in the case of Pt/CeO_2(111). Strong features around 284.8 eV indicate the existence of CH_x (x = 1, 2, and 3) species formed by the partial dissociation of methane {$CH_4 \rightarrow CH_x + (4\text{-}x)$ H} on the surface.[18−20] A second peak located near 290 eV points to the formation of carbonate-like CO_x species as a final product of the full decomposition of methane.[18−20] The Pt/CeO_2(111) surfaces in Figure 2 exhibit a reactivity toward methane higher

https://dx.doi.org/10.1021/acscatal.0c04694
ACS Catal. 2021, 11, 1613−1623

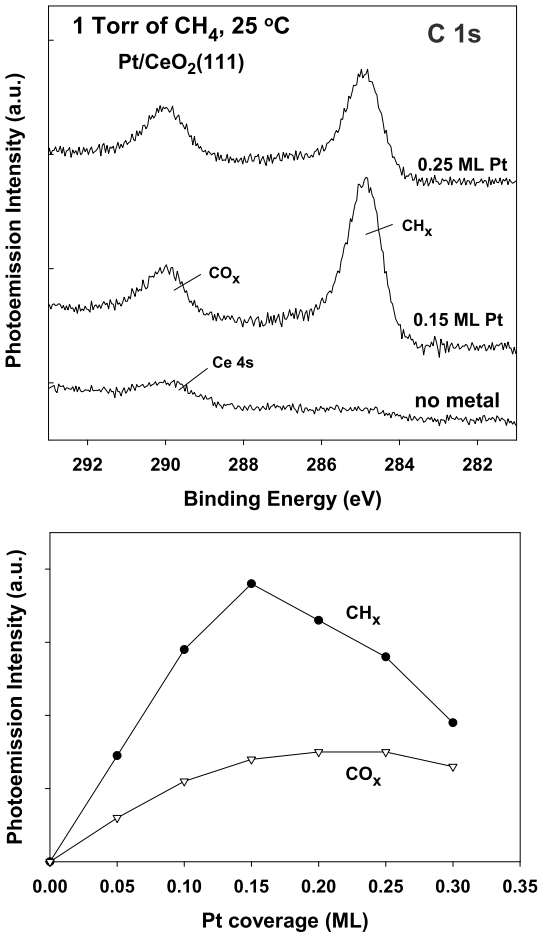

Figure 2. Top panel: C 1s XPS spectra collected after exposing plain $CeO_2(111)$ and $Pt/CeO_2(111)$ surfaces to 1 Torr of methane at 25 °C for 5 min. Bottom panel: Variation in the signal for CH_x and CO_x species in the C 1s region as a function of admetal coverage in $Pt/CeO_2(111)$.

than that seen for surfaces of the bulk metal such as Pt(111), Pt(100), or Pt(110)-(1×2).[31−34]

The reactivity of the $Pt/CeO_2(111)$ surfaces to dissociate methane at 25 °C depended strongly on the amount of platinum dispersed on ceria. The highest reactivity was seen for the system with 0.15 ML (see Figure 2). This correlates with the large electronic perturbations seen in valence photoemission (Figure 1). At higher coverages of Pt (> 0.2 ML), the electronic perturbations on Pt decreased,[37] and the amount of CH_x and CO_x deposited on the surface upon exposure also dropped (bottom panel in Figure 2). Previous theoretical studies have indicated that electronic perturbations associated with Pt-CeO_2 bonding can largely reduce the barrier for the activation of C−H bonds in methane.[42]

Figure 3 displays C 1s XPS spectra acquired after dosing 1 Torr of CO_2 to clean $CeO_2(111)$ and an oxide surface precovered with 0.15 ML of platinum at 25 °C. For both systems, the adsorption of CO_2 produces a peak around 290 eV which can be assigned to a carbonate (CO_x) species produced by direct reaction of CO_2 with O sites of the surface.[18−20] The presence of Pt did not lead to the growth of clear peaks for adsorbed CO_2 or CO on the metal, but the occurrence of a reaction of the CO_2(gas) → CO(gas) + O(surface) type cannot be ruled out. XPS results showed that platinum was oxidized from mainly Pt^{1+} to Pt^{2+} upon exposure

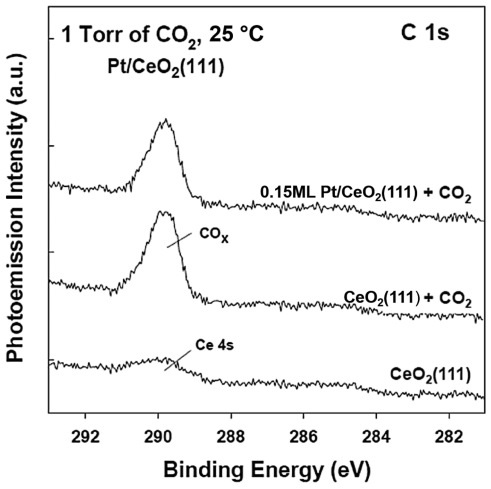

Figure 3. C 1s XPS spectra collected after exposing plain $CeO_2(111)$ and a $Pt/CeO_2(111)$ surface to 1 Torr of CO_2 at 25 °C for 5 min. The carbonate (CO_x) peak did not disappear when the surface was heated to temperatures as high as 500 °C.

to CO_2. This is remarkable because neither Pt(111) nor Pt(100) bind carbon dioxide well.[7] The similarities of the carbonate peaks in Figure 3 suggest that the adsorbed CO_2 mainly interacted with the ceria support. Thus, our XPS results indicated that CH_4 and CO_2 can be adsorbed on $Pt/CeO_2(111)$ at room temperature, but they did not react to yield syngas as expected by the MDR process. Catalytic activity was observed at temperatures above 400 °C after methane reduced ceria producing O vacancies where CO_2 dissociated.

A batch reactor was used to test the catalytic performance of plain Pt(111), $CeO_2(111)$, and 0.15 ML of Pt deposited on a $CeO_2(111)$ surface. At the reaction conditions examined (1 Torr of CH_4, 1 Torr of CO_2, 400−500 °C), neither Pt(111) nor $CeO_2(111)$ showed any sustained activity for the MDR reaction. In the case of Pt(111), some catalytic activity was initially observed but it dropped continuously and, after 20 min of reaction, no catalytic activity was seen (Figure 4). Postreaction characterization with XPS showed that the plain

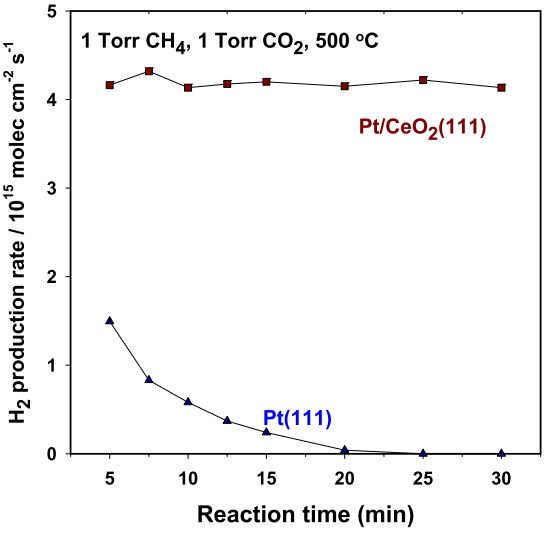

Figure 4. Production of H_2 by methane dry reforming on Pt(111) and 0.15 ML of Pt supported on $CeO_2(111)$. Reaction conditions: 1 Torr of CH_4, 1 Torr of CO_2, and 500 °C.

https://dx.doi.org/10.1021/acscatal.0c04694
ACS Catal. 2021, 11, 1613−1623

platinum surface was poisoned by a thick carbon layer generated by the decomposition of methane. On this system, CO_2 could not dissociate fast enough to provide the O for the removal of the carbon generated by methane.[32] In addition, Pt(111) is known to be active for the Boudouard reaction ($2CO \rightarrow C + CO_2$) which also could induce platinum deactivation by carbon poisoning.

In contrast to the behavior of Pt(111), our kinetic data shown in Figure 4 indicate that a catalyst generated by depositing 0.15 ML of Pt on a CeO_2(111) surface is highly active and stable for the MDR reaction. The metal−support interactions in the Pt-CeO_2 interface lead to an excellent catalytic performance. Furthermore, these interactions also substantially reduce the rate of the Boudouard reaction with respect to Pt(111).[37] Thus, both factors make Pt/CeO_2(111) a very good catalyst for the MDR process. Postreaction characterization with XPS gave a negligible amount of C on Pt/CeO_2(111) after 30 min of reaction under MDR conditions. In the C1s XPS region, a peak for carbonate, similar to that seen in Figure 3, was seen. Furthermore, upon finishing the postreaction characterization with XPS, the sample was transferred back to the reactor and the MDR process was performed under the same conditions as those shown in Figure 4 for an additional 2 h, observing the same rate of H_2 production and no measurable deposition of carbon on the surface of the catalyst.

Figure 5 displays the calculated turnover frequency (TOF) at 500 °C for different Pt/CeO_2(111) systems as a function of

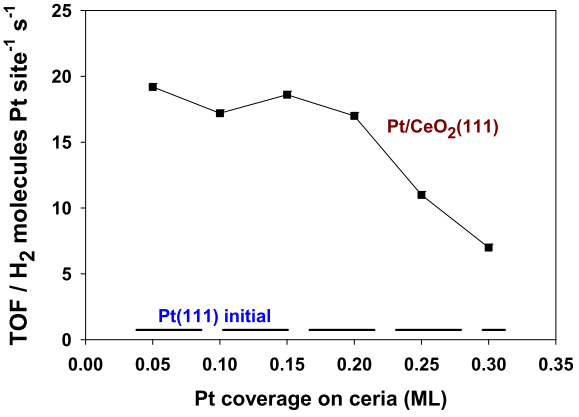

Figure 5. Calculated turnover frequencies for Pt/CeO_2(111) surfaces. For comparison, the initial TOF of Pt(111), before it was deactivated by carbon deposition, is included as the dashed line at the bottom. Reaction conditions: 1 Torr of CH_4, 1 Torr of CO_2, and 500 °C.

admetal coverage. The TOFs were calculated assuming that all the Pt atoms which were present on the ceria support were active in the catalytic process. For comparison, as shown in Figure 5, we also include the initial TOF for Pt(111) before its surface was deactivated by carbon deposition. Results shown in Figure 5 indicate that at small coverages of Pt, the dispersed particles on ceria are at least 20 times more active than plain Pt(111). Thus, the remarkable increase in the activity and stability of Pt might be linked to the strong interactions of small coverages of Pt with CeO_2. As shown in Figure 5, the TOF decreases when the Pt coverage goes above 0.2 ML—a phenomenon which correlates with a reduction in the electronic perturbations[37] in Pt and in the reactivity of the admetal toward methane (Figure 2).

Ambient pressure-XPS (AP-XPS) was used to study the chemical state of a Pt/CeO_2(111) catalyst when exposed to a reactant CH_4/CO_2 mixture in a large range of temperature (Figure 6). The initial position of the Pt 4f peak indicates that

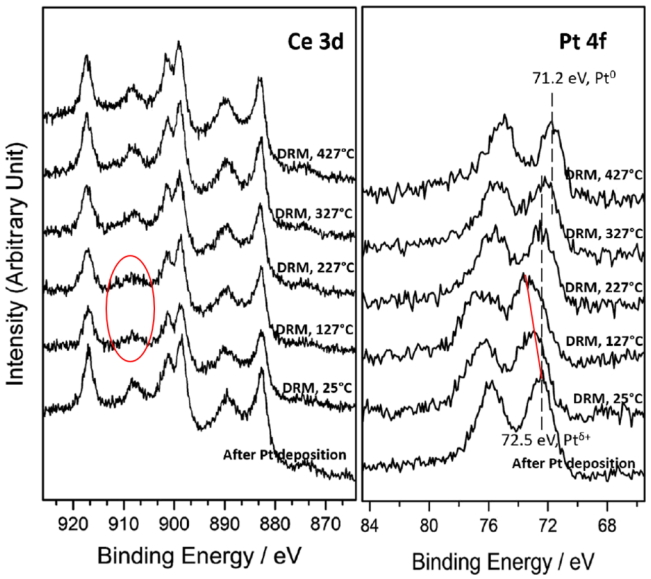

Figure 6. Ce 3d and Pt 4f AP-XPS spectra of Pt/CeO_2 (111) for the MDR reaction at elevated temperatures. Spectra were collected at 25, 127, 227, 327, and 427 °C in a 50 mTorr CH_4 + 50 mTorr CO_2 gas atmosphere.

Pt is oxidized with a Pt^+-dominating feature upon deposition on CeO_2(111) at 25 °C.[40−42] The exposure to the CH_4 and CO_2 gas mixture induced a peak shift of the Pt signal to higher binding energy at 25 and 127 °C. This peak shift could be attributed to the adsorbed CO_x/CH_x species (resulting from CH_4 dissociation and CO_2 binding, see Figures 2 and 3) on the Pt surface which increased the work function and binding energy.[43,44] An analysis of the corresponding Ce 3d XPS spectra indicates that there may be some reduction of Ce^{4+} into Ce^{3+} upon exposure to the CH_4/CO_2 gas mixtures at different temperatures. As can be seen, upon deposition of Pt, most of the ceria is in the 4+ state, and the decline of the Ce^{4+} $3d_{3/2}$ signal (peak at ∼909 eV) at 25 and 127 °C under the MDR reaction condition indicates a slight reduction of Ce^{4+}. This phenomenon was not observed on other similar 0.15 ML M/CeO_2(111) (M = Co, Ni, and Cu) catalysts,[19] implying a much stronger metal−support interaction in the Pt/CeO_2(111) system. In addition, the slight reduction observed on the ceria support at 25 °C also manifests the increased reducibility of ceria when Pt was loaded, as there is no sign for CH_4 dissociation on pure CeO_2 at 25 °C as shown in Figure 2. This increased reducibility was also verified on the Pt/CeO_2 powder system, as can be seen in Figure S1; the loading of Pt on the ceria support significantly decreased the temperature needed to reduce the surface of ceria.

As seen in Figure 6, as the temperature increases, a total shift of the Pt signal to lower binding energy at 327 and 427 °C was observed in the AP-XPS spectra, indicating the reduction of $Pt^{\delta+}$, and under the active MDR reaction conditions (> 400 °C), metallic Pt is present in the surface of the catalyst.[40,41] The Ce^{4+} peak (at ∼909 eV) also grows at 227 °C and the signal of Ce^{3+} is negligible until 427 °C under the MDR reaction condition.[45] In test experiments, we found that plain

https://dx.doi.org/10.1021/acscatal.0c04694
ACS Catal. 2021, 11, 1613−1623

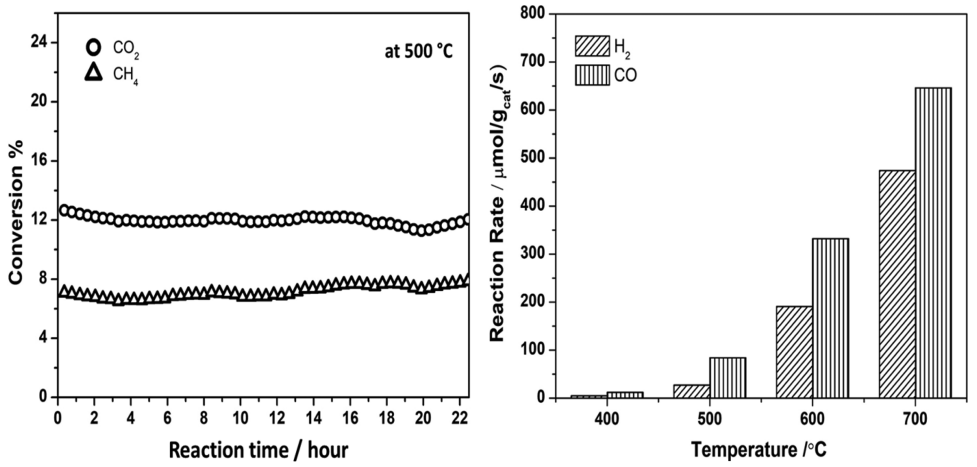

Figure 7. Catalytic performance of the 0.5 wt % Pt/CeO_2 catalyst for the MDR reaction at different temperatures (400−700 °C).

methane reduces ceria in the $Pt/CeO_2(111)$ system at elevated temperatures (~23% of Ce^{4+} was reduced to Ce^{3+} at 427 °C, see Figure S2 and Table S1), but the formed Ce^{3+} quickly reoxidized to Ce^{4+} upon exposure to CO_2. This indicates that a balanced redox cycle was achieved on the ceria support when the sample was exposed to the MDR reaction atmosphere. In general, under the active MDR reaction conditions, an interface containing small particles of Pt dispersed on a reactive ceria support is the active phase of the MDR catalyst.

Reaction of CH_4 and CO_2 on Pt/CeO_2 Powder. Previous studies of AP-XPS and time-resolved X-ray diffraction (XRD) have shown that Pt/CeO_2 powder is also effective for the low temperature activation of methane.[42] Thus, we decided to test such a system in the conversion of CO_2/CH_4 and investigate the possible metal−support interactions in the Pt/CeO_2 powder system under the MDR reaction condition. Tests in a flow reactor showed that a 0.5 wt % Pt/CeO_2 powder was active and stable as an MDR catalyst at 500 °C with a very good performance at even higher temperatures (Figure 7). In the tests shown in Figure 7, CO_2 was consumed by the MDR and reverse water-gas shift ($CO_2 + H_2 \rightarrow CO + H_2O$) reactions. At 500 °C, there was a 7% conversion of CH_4 and 13% conversion of CO_2, with the system remaining stable for more than 20 h. The production rate of H_2 and CO was 27 and 84 μmol/g_{cat}/s, respectively, at 500 °C and reached to 475 and 650 μmol/g_{cat}/s at 700 °C.

A combination of in situ measurements with AP-XPS, X-ray absorption fine structure (XAFS), and XRD was used to fully characterize the 0.5 wt % Pt/CeO_2 powder catalyst under reaction. The AP-XPS results are summarized in Figure 8. Any $Pt^{\delta+}$ feature present on the samples at 25 °C was prereduced in H_2 so that active metallic Pt was present on the catalysts surface for the MDR process. The prereduced Pt^0 maintains its metallic feature throughout the MDR reaction at elevated temperatures. In the Ce 3d XPS region, the pretreatment process induced a partial reduction of Ce^{4+} to Ce^{3+}; however, after switching gas to the MDR reaction gas mixture at 25 °C, part of Ce^{3+} was reoxidized back to Ce^{4+} by CO_2, and under the reaction conditions, Ce^{4+} and Ce^{3+} kept a relatively stable ratio at elevated temperatures. On the surface of this catalyst, probably a dynamic redox process occurred under the MDR reaction conditions, where methane or H produced by methane dissociation reduced some Ce^{4+} to Ce^{3+}, which was then partially reoxidized back by the dissociation of CO_2.

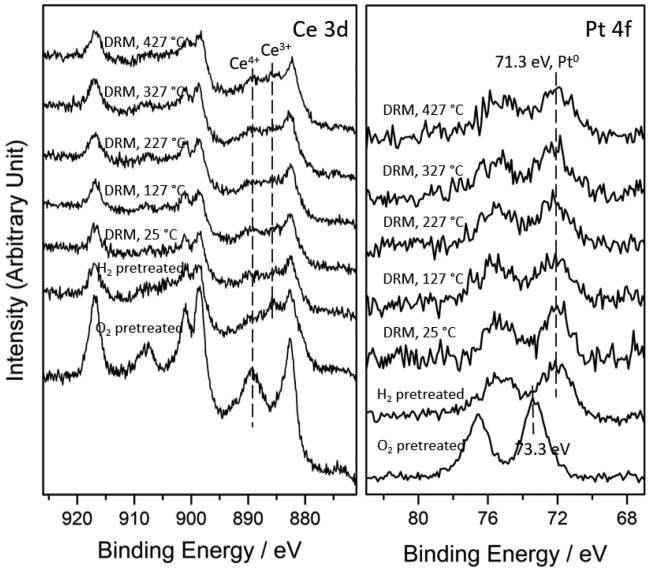

Figure 8. Ce 3d and Pt 4f AP-XPS spectra of 0.5 wt % Pt/CeO_2 for the MDR reaction at elevated temperatures. A 10 mTorr O_2 and a 20 mTorr of H_2 were used to pretreat the sample at 400 °C sequentially to remove the surface-bounded carbon species and reduce the sample, respectively.

A reduction of the supported platinum was also observed in X-ray absorption near edge structure (XANES) and extend X-ray absorption fine structure (EXAFS) measurements collected for the powder Pt/CeO_2 catalyst using a flow reactor and the regular conditions for the MDR process. The Pt L_3 edge XANES and the Fourier transformed EXAFS spectra are presented in Figure 9. PtO_2 (Pt^{4+}) was identified as a dominant structure in the as-prepared Pt/CeO_2 powder sample,[46−48] see Figure 9a. The strong Pt-O feature in the EXAFS spectrum of the pristine sample which aligns with the Pt-O characteristic peak of the PtO_2 reference also confirms the initial presence of PtO_2 in the bulk.[49] After H_2 reduction, PtO_2 was converted to metallic Pt, which remained until 700 °C under the MDR reaction. In Figure 9b, a peak shift of ~0.19 Å in the Pt-Pt shell was observed for the H_2 pretreated sample and the sample under MDR conditions. This leftward shift implies shorter Pt−Pt bond distance of the small Pt clusters when they are supported on ceria, which evidenced the modification of Pt by

https://dx.doi.org/10.1021/acscatal.0c04694
ACS Catal. 2021, 11, 1613−1623

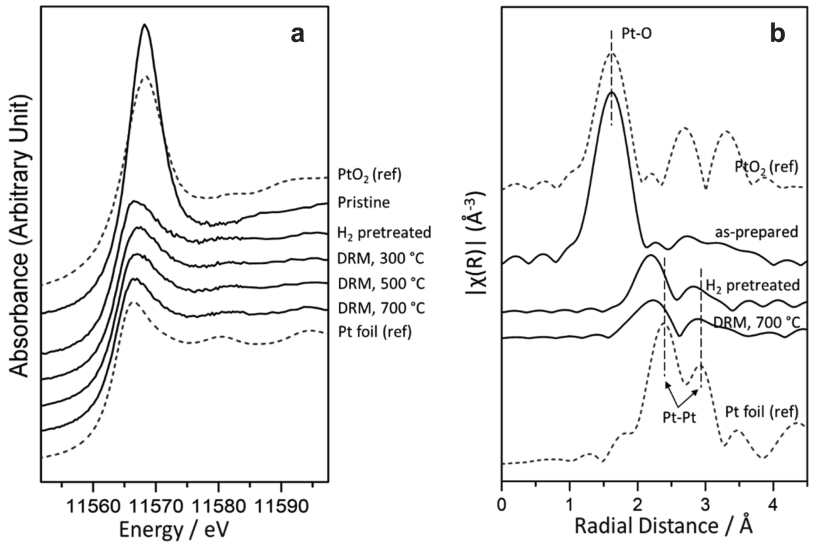

Figure 9. Pt L_3 in situ XANES (a) and the Fourier transformed EXAFS region (b) of the sample during the MDR reaction at different temperatures. For comparison, we also include data for Pt foil and PtO_2 powder.

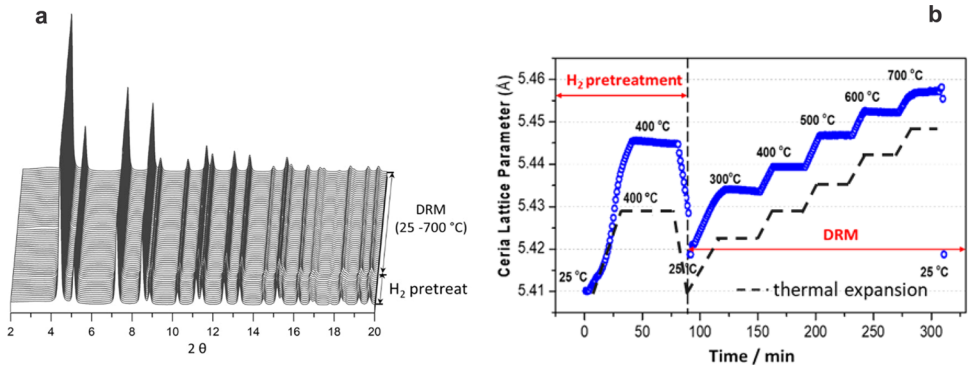

Figure 10. (a) Time-resolved in situ XRD profile of Pt/CeO_2 and (b) evolution of the ceria lattice parameter during the MDR reaction.

the ceria support through the metal−support interactions in the powder Pt/CeO_2 system.

Figure 10 shows in situ XRD data for 0.5 wt % Pt/CeO_2 under the MDR process. Only diffraction features for ceria are observed in Figure 10a because the Pt particles are too small (< 2 nm) to yield diffraction lines. Rietveld refinement allowed us to track variations in the ceria lattice (Figure 10b). The XRD measurements point to an expansion of the ceria lattice indicating a reduction of the ceria support, which is also consistent with the existence of some Ce^{3+} in the powder catalyst as seen in AP-XPS (Figure 8). The ceria support was partially reduced by H_2 with a 0.02 Å lattice expansion (from 5.41 to 5.43 Å) during the H_2 pretreatment process. After switching the feed from H_2 to an MDR reaction gas mixture at 25 °C, the ceria lattice decreased to 5.42 Å, indicating the partial reoxidation of the ceria support by CO_2 at room temperature. Under the MDR reaction conditions, the ceria lattice expanded at elevated temperatures, following the thermal expansion trend of ceria, and after cooling down the sample to 25 °C, the ceria lattice contracted back to the same value as before the MDR reaction. When compared to the total lattice expansion of ceria under a pure CH_4 gas environment from 25 to 700 °C (0.11 Å, in additional test measurements, shown in Figure S3), this result suggests that the partial reduction of the ceria support preserved a stable Ce^{3+} to Ce^{4+} ratio under the MDR reaction conditions (consistent with the results shown in Figure 8), and this implied that a balanced redox process, induced by simultaneous CH_4 and CO_2 decomposition, was achieved on the ceria support. This balanced redox process, also observed on the $PtCeO_2(111)$ model catalyst, is essential for the catalytic reaction. Although both reactants adsorb on the catalyst surface at 25 °C (Figures 2 and 3), a stable catalytic cycle is only established at elevated temperatures when methane or H produced by the dissociation of methane is able to reduce the ceria-forming Ce^{3+} sites which are effective for the dissociation of CO_2.

Comparison to Other Metal/Oxide Catalysts for the MDR Process. Small particles of Pt in contact with ceria display special electronic properties (valence photoemission data, Figure 1) and shorter Pt−Pt distances (EXAFS data, Figure 9) with respect to bulk Pt. These results are consistent with findings of previous studies examining the interaction of Pt atoms or small metal clusters with ceria.[35−37,45] The electronic and structural perturbations affect the reactivity of the supported Pt particles. The results discussed above illustrate the cooperative interactions which can occur when a metal-oxide interface is used for the activation of CH_4 and CO_2 in a dry reforming process.

In general, surfaces of pure platinum are not efficient for the activation of methane or carbon dioxide.[7,32−34] The metal component alone cannot carry out the chemistry, and the oxide modifies the catalytic properties of the metal and

https://dx.doi.org/10.1021/acscatal.0c04694
ACS Catal. 2021, 11, 1613−1623

participates in key reaction steps. In principle, the catalytic properties of the metal-oxide interface can be altered by changing its metal or oxide components. Figure 11 compares

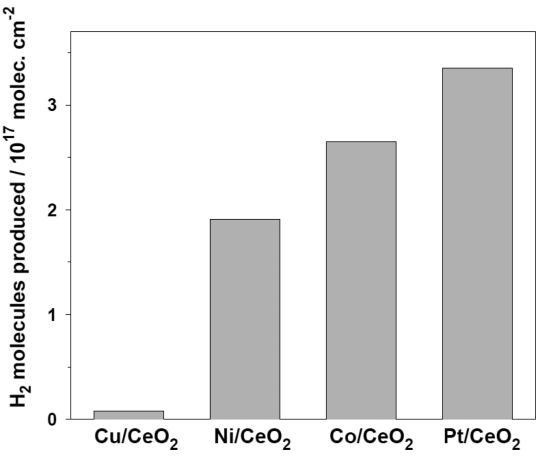

Figure 11. Catalytic activity for MDR on Cu-, Ni-, Co-, and Pt/CeO_2 catalysts (~0.15 ML of admetal). Amounts of H_2 formed after exposing the catalysts to 1 Torr of CH_4 and 1 Torr of CO_2 at 650 K for 5 min.

the catalytic activity of Pt/CeO_2(111) and a series of M/CeO_2(111) surfaces (M = Cu, Ni, or Co) at an admetal coverage of ~0.15 ML.[18−20] The high activity of Ni/CeO_2 is remarkable;[50−52] however, the surfaces with Co and Pt are clearly the best catalysts, with Pt being more selective than Co since it does not form ethane or ethylene during the MDR process, as it is the case with Co.[19] Thus, in Pt/CeO_2, one has the best metal-ceria system with high activity, stability, and selectivity.

In general, when optimizing the performance Pt MDR catalysts, scientists have followed two different approaches: changing the oxide support (Al_2O_3, MgO, CeO_2, ZrO_2, and CeO_2-ZrO_2) and alloying Pt with a second metal (Fe, Co, Ni, and Cu).[6,25−29,53−55] Our results show the important role that ceria plays as an active support/participant in the MDR process. It is superior with respect to Al_2O_3 and MgO because these oxides usually do not interact strongly with supported metals like ceria does. Pure ZrO_2 does interact with metals and produces an active ZrO_2/Pt interface for the MDR reaction,[53] but it does not have the redox properties of ceria which facilitate the dissociation of CO_2 and its incorporation within a catalytic cycle. On the other hand, zirconia-doped ceria is an interesting support because it interacts well with metals and its redox properties (Ce^{4+} to Ce^{3+} switching) could be enhanced with respect to plain ceria; the increased stability against filamentous coke formation has also been reported on a Ni-based catalyst.[6,25,27,54,55]

Typically, surfaces of pure platinum {Pt(111), Pt(100), or Pt(110)-(1×2)} interact poorly with methane and, at high temperatures in which the breaking of C−H bonds is efficient, they become rapidly covered by a carbonaceous layer which leads to chemical and catalytic deactivation.[31−34] The formation of metal−metal interfaces, or alloys, is an approach which is frequently used to prevent coke generation and subsequent deactivation during the MDR process.[6,8] Pt is usually alloyed with a second metal (Ni, Co, Rh, Ru, or Ir) to increase the activity of the system for CO_2 dissociation or to prevent carbon deposition and catalyst deactivation.[6,25,26,28,29] In our Pt/CeO_2 system, only a very small amount of Pt (0.15 ML and 0.5 wt %) was needed, and the chemical performance of the metal was promoted by interactions with the active oxide support, with ceria also helping in the dissociation of CO_2. The results shown in Figures 2 and 3 are really remarkable because the common alloys of Pt investigated so far have not been able to bind CO_2 and CH_4 well or activate them in an effective way at room temperature.[6,25−29,56,57] The TOFs seen in Figure 5 (17−19 H_2 molecules produced site^{-1} s^{-1}) are much larger than typical TOFs obtained after alloying Pt with a second metal (2−5 H_2 molecules produced site^{-1} s^{-1}).[29,58,59] Thus, optimizing metal−support interactions and using an active oxide support seem a much more efficient approach than plain bimetallic bonding when one wants to produce a highly active, selective, and stable catalyst for the MDR process.

CONCLUSIONS

Pt(111) reacts poorly with carbon dioxide and methane. Elevated temperatures are necessary to activate these molecules, and a massive deposition of carbon made this pure metal surface useless for the MDR process. The deposition of small Pt particles on ceria produces systems with short Pt−Pt distances and induces large electronic perturbations in the valence states of the admetal, evidencing strong metal−support interactions in Pt/CeO_2(111) and Pt/CeO_2 powders, leading to systems which bind CO_2 and CH_4 well at room temperature and are excellent and stable catalysts for the MDR process at moderate temperatures (500 °C). Studies with in situ or *operando* methods (AP-XPS, XRD, and XAFS) point to an active Pt-CeO_{2-x} interface. In this interface, the oxide is not only a passive spectator but also modifies the chemical properties of Pt, facilitating methane dissociation, and is directly involved in the adsorbing and dissociation of CO_2, making the MDR catalytic cycle possible. A comparison of the benefits gained by the use of an effective metal-oxide interface and those obtained by plain bimetallic bonding indicates that the former is much more important when optimizing the C1 chemistry associated with CH_4 and CO_2 conversion. The presence of elements with a different chemical nature at the metal-oxide interface opens up the possibility for truly cooperative interactions in the activation of C−H and C−O bonds.

METHODS

Studies with Well-Defined Pt/CeO_2(111) Surfaces. The experiments examining the activation of CH_4 and its conversion by reaction with CO_2 on Pt/CeO_2(111) surfaces were performed in a setup that combined an ultrahigh vacuum (UHV) chamber for surface characterization and a micro-reactor for catalytic tests.[18,19,37] The UHV chamber was equipped with instrumentation for XPS, low-energy electron diffraction, ion-scattering spectroscopy, and thermal-desorption mass spectroscopy.[18,19,37] The methodology followed for the preparation of the Pt/CeO_2(111) surfaces is described in detail in ref.[37] For Pt/CeO_2(111) surfaces, single atoms and small Pt clusters have been observed at low coverages using scanning tunneling microscopy.[60] In the studies of methane activation, the sample was transferred in vacuo to the reactor at 25 °C and then the reactant gas, 1 Torr of pressure, was introduced. In the experiments of testing the activity of Pt(111) and Pt/CeO_2(111) catalysts for the MDR reaction, the samples were under a gas mixture of 1 Torr of CH_4 and 1

https://dx.doi.org/10.1021/acscatal.0c04694
ACS Catal. 2021, 11, 1613−1623

Torr of CO_2 at room temperature and were heated in a fast ramp to a reaction temperature of 500 °C. The MDR products were analyzed by mass spectroscopy or gas chromatography. In our catalytic experiments, yields were measured at intervals of 5 min. For each run, the number of molecules (CO and/or H_2) generated in the kinetic tests was normalized by the active area exposed by the sample and the total reaction time. All these kinetic experiments in a batch reactor were done under a limit of low conversion (< 10%).

AP-XPS measurements were carried out on a commercial SPECS AP-XPS chamber equipped with a PHOIBOS 150 EP MCD-9 analyzer at the Chemistry Division of Brookhaven National Laboratory (BNL). In the preparation of the Pt/CeO_2(111) model catalyst, the Ce metal was first evaporated onto a Ru single crystal (0001) at 427 °C in the presence of 5×10^{-7} torr O_2 and then annealed to 527 °C for 10 mins at the same O_2 pressure. The ceria films were estimated to be ca. 4 nm thick (≈10 layers of O-Ce-O) based on the attenuation of the Ru 3d XPS signal. Pt was vapor-deposited on the as-prepared ceria film at 427 °C, and the coverage of Pt was ~0.15 ML, estimated by the attenuation of the Ce 3d XPS signal. In the studies of MDR on the Pt/CeO_2(111) catalyst, a 50 mTorr CH_4 and 50 mTorr CO_2 gas mixture was used and Ce 3d and Pt 4f spectra were collected at 25, 127, 227, 327, and 427 °C. The binding energies in the AP-XPS spectra were calibrated using the strongest Ce^{4+} 3d feature located at 916.9 eV as a reference.

Studies with Pt/CeO_2 Powder Catalysts. *Catalyst Preparation.* Cerium oxide (CeO_2) was prepared by precipitating white crystalline cerous nitrate ($Ce(NO_3)_3.6H_2O$; Sigma-Aldrich), dissolved in deionized water with mild stirring. The temperature was kept at 100 °C and ammonia (0.91 $molL^{-1}$) was added dropwise until a pH of 8 was attained. The resulting white slurry precipitate was then collected by filtration, washed with deionized water, and left to dry in an oven at 100 °C for 12 h. The pale purple dried powder was calcined in a furnace at 500 °C for 4 h with flowing air. The sample was then ground but not sieved to a consistent powder with a mortar and pestle. The required amount of Pt to make 0.5 wt % Pt/CeO_2 (0.05 g of Pt on 9.95 g of CeO_2) was deposited on CeO_2 by impregnation from a stock solution of 1 L/g of Pt cations (from $PtCl_4$—Sigma-Aldrich) in a beaker at ambient temperature with continuous stirring. The temperature of the beaker was then raised to around 100 °C, while stirring, and retained at this temperature until most of the liquid has vaporized (the complete impregnation process takes about 6−8 h) to form a pastelike material, which was then dried in an oven for 12 h at 100 °C to remove the remaining water. The dried powder was then calcined in a furnace for 4 h at 400 °C under flowing air.

Catalytic Performance. In the catalytic test for the (0.5 wt %) Pt/CeO_2 powder catalyst under the MDR reaction, a sample of ~12.5 mg was loaded into a quartz tube flow reactor for the measurements. The catalysts were pretreated with H_2 at 400 °C for 40 min to generate active metallic Pt and then an MDR reaction gas mixture (10 cc/min CH_4, 10 cc/min CO_2, and 10 cc/min N_2) was switched into the flow system for the reaction test. The weight hourly space velocity was 180,000 $mL/g_{cat}/h$. The catalysts were heated to 700 °C with a 10 °C/min ramping rate and isothermal stages at 400, 500, 600, and 700 °C, and at each temperature stage, the soak time was 1 h. A residual gas analyzer and a gas chromatography instrument (Agilent 7890A) were connected to the end of the flow reactor to analyze the reaction gas products and the catalytic activity was measured and calculated at each of the isothermal stages (400, 500, 600, and 700 °C) investigated.

XAFS. In situ XANES and EXAFS for the MDR reaction on Pt/CeO_2 were recorded at 9BM of the Advanced Photon Source (APS), at Argonne National Laboratory (ANL). Around 2 mg of the catalysts was loaded into a Clausen cell flow reactor and directly placed in front of the synchrotron X-rays for the in situ measurement. The catalysts were pretreated in H_2 at 400 °C for 40 min before switching to a 2 cc/min CH_4, 2 cc/min CO_2, and 6 cc/min He gas mixture for the MDR reaction testing. The catalysts were then heated to 700 °C with a 10 °C/min ramping rate and the Pt L_3-edge spectra were collected in the fluorescence yield mode at temperature stages of 300, 500, and 700 °C by a four channel Vortex detector. At least three spectra at each temperature stage were collected and averaged to improve the data quality, and these spectra were further processed using the IFEFFIT package.[61]

AP-XPS. The powder catalyst was pressed onto an aluminum plate and loaded on a sample holder in the AP-XPS chamber. A 10 mTorr of O_2 was introduced and the sample was heated to 400 °C to remove any surface-bounded carbon species before the test. In the studies of MDR on the Pt/CeO_2 powder catalyst, the sample was prereduced in a 20 mTorr of H_2 at 400 °C for 40 min before switching to a 50 mTorr CH_4 and 50 mTorr CO_2 reaction gas mixture. The Pt 4f and Ce 3d XPS signals were collected at 25, 127, 227, 327, and 427 °C.

XRD. A Clausen cell flow reactor was used for the in situ time-resolved XRD studies.[62] The measurements were conducted at the 17BM beamline of the Advanced Photon Source (APS), at Argonne National Laboratory (ANL), with an X-ray wavelength at 0.24108 Å. The reaction conditions were kept the same as those for the in situ XAFS measurements. Two-dimensional XRD images were continuously collected by an amorphous Si flat panel (PerkinElmer) detector throughout the reaction process and the XRD images were further processed with the GSAS-II code to generate XRD patterns (Intensity versus 2θ). The lattice parameter evolution of ceria was calculated by Rietveld refinement also using GSAS-II.[63] Pt particles or aggregates were not seen in XRD and TEM for the 0.5 wt % Pt/CeO_2 powder catalyst. The use of low loading is crucial for the comparison of model systems with high surface area catalysts and for defining structure−function relationships.[64]

■ ASSOCIATED CONTENT

Supporting Information

The Supporting Information is available free of charge at https://pubs.acs.org/doi/10.1021/acscatal.0c04694.

The H_2 TPR results on the Pt/CeO_2 powder sample and bare ceria support; AP-XPS signal and the peak fitting at the Ce 3d region of 0.15 ML Pt/CeO_2(111) under a pure CH_4 atmosphere at 427 °C; fitting parameters and results of the Ce 3d spectrum; ceria lattice parameter evolution in a CH_4 atmosphere as a function of temperature (PDF)

■ AUTHOR INFORMATION

Corresponding Authors

M. Verónica Ganduglia-Pirovano − *Instituto de Catálisis y Petroleoquímica, CSIC, Madrid 28049, Spain;* orcid.org/0000-0003-2408-8898; Email: vgp@icp.csic.es

https://dx.doi.org/10.1021/acscatal.0c04694
ACS Catal. 2021, 11, 1613−1623

Sanjaya D. Senanayake − *Chemistry Division, Brookhaven National Laboratory, Upton, New York 11973, United States;* orcid.org/0000-0003-3991-4232; Email: ssenanay@bnl.gov

José A. Rodriguez − *Department of Materials Science and Chemical Engineering, SUNY at Stony Brook, Stony Brook, New York 11794, United States; Chemistry Division, Brookhaven National Laboratory, Upton, New York 11973, United States;* orcid.org/0000-0002-5680-4214; Email: rodrigez@bnl.gov

Authors

Feng Zhang − *Department of Materials Science and Chemical Engineering, SUNY at Stony Brook, Stony Brook, New York 11794, United States*

Ramón A. Gutiérrez − *Facultad de Ciencias, Universidad Central de Venezuela, Caracas 1020-A, Venezuela*

Pablo G. Lustemberg − *Instituto de Física Rosario (IFIR), CONICET-UNR, Rosario, Santa Fe S2000EZP, Argentina; Instituto de Catálisis y Petroleoquímica, CSIC, Madrid 28049, Spain*

Zongyuan Liu − *Chemistry Division, Brookhaven National Laboratory, Upton, New York 11973, United States*

Ning Rui − *Chemistry Division, Brookhaven National Laboratory, Upton, New York 11973, United States*

Tianpin Wu − *X-ray Science Division, Advanced Photon Source, Argonne National Laboratory, Argonne, Illinois 60439, United States*

Pedro J. Ramírez − *Facultad de Ciencias, Universidad Central de Venezuela, Caracas 1020-A, Venezuela; Zoneca-CENEX, R&D Laboratories, Alta Vista, Monterrey 64770, México*

Wenqian Xu − *X-ray Science Division, Advanced Photon Source, Argonne National Laboratory, Argonne, Illinois 60439, United States;* orcid.org/0000-0002-4815-6253

Hicham Idriss − *SABIC Corporate Research & Development (CRD), KAUST, Thuwal 29355, Saudi Arabia*

Complete contact information is available at: https://pubs.acs.org/10.1021/acscatal.0c04694

Notes

The authors declare no competing financial interest.

The data that support the plots presented in this paper and other findings of this study are available from the corresponding authors on reasonable request.

■ ACKNOWLEDGMENTS

The research carried out at the Brookhaven National Laboratory (BNL) was supported by the U.S. Department of Energy, Office of Science and Office of Basic Energy Sciences under contract No. DE-SC0012704. The XRD and XAFS experiments carried out at the Advanced Photon Source Beamline 17BM (XRD) and 9BM (XAFS) at Argonne National Laboratory was supported by the U.S. DOE under Contract No. DE-AC02-06CH11357. This project has also received funding from the European Union's Horizon 2020 research and innovation programme under the Marie Skłodowska-Curie grant agreement No 832121. M.V.G.P. thanks the support from the MINECO and MICINN-Spain (CTQ2015-71823-R and RTI2018-101604-B-I00, respectively).

■ REFERENCES

(1) Anderson, T. R.; Hawkins, E.; Jones, P. D. CO_2, the greenhouse effect and global warming: from the pioneering work of Arrhenius and Callendar to today's Earth System Models. *Endeavour* **2016**, *40*, 178−187.

(2) Schwarz, H.; Shaik, S.; Li, J. Electronic Effects on Room-Temperature, Gas-Phase C−H Bond Activations by Cluster Oxides and Metal Carbides: The Methane Challenge. *J. Am. Chem. Soc.* **2017**, *139*, 17201−17212.

(3) Thornton, P. K. Livestock production: recent trends, future prospects. *Philos. Trans. R. Soc. Lond. B. Biol. Sci.* **2010**, *365*, 2853−2867.

(4) Tang, P.; Zhu, Q.; Wu, Z.; Ma, D. Methane activation: the past and future. *Energy Environ. Sci.* **2014**, *7*, 2580−2591.

(5) Bousquet, P.; Ciais, P.; Miller, J. B.; Dlugokencky, E. J.; Hauglustaine, D. A.; Prigent, C.; Van der Werf, G. R.; Peylin, P.; Brunke, E. G.; Carouge, C.; Langenfelds, R. L.; Lathière, J.; Papa, F.; Ramonet, M.; Schmidt, M.; Steele, L. P.; Tyler, S. C.; White, J. Contribution of anthropogenic and natural sources to atmospheric methane variability. *Nature* **2006**, *443*, 439−443.

(6) Arora, S.; Prasad, R. An overview on dry reforming of methane: strategies to reduce carbonaceous deactivation of catalysts. *RSC Adv.* **2016**, *6*, 108668−108688.

(7) Liu, X.; Sun, L.; Deng, W.-Q. Theoretical Investigation of CO2 Adsorption and Dissociation on Low Index Surfaces of Transition Metals. *J. Phys. Chem. C* **2018**, *122*, 8306−8314.

(8) Song, Y.; Ozdemir, E.; Ramesh, S.; Adishev, A.; Subramanian, S.; Harale, A.; Albuali, M.; Fadhel, B. A.; Jamal, A.; Moon, D.; Choi, S. H.; Yavuz, C. T. Dry reforming of methane by stable Ni−Mo nanocatalysts on single-crystalline MgO. *Science* **2020**, *367*, 777−781.

(9) Vogt, C.; Monai, M.; Sterk, E. B.; Palle, J.; Melcherts, A. E.; Zijlstra, B.; Groeneveld, E.; Berben, P. H.; Boereboom, J. M.; Hensen, E. J. Understanding carbon dioxide activation and carbon−carbon coupling over nickel. *Nat. Commun.* **2019**, *10*, 1−10.

(10) Weaver, J. F.; Hakanoglu, C.; Antony, A.; Asthagiri, A. Alkane activation on crystalline metal oxide surfaces. *Chem. Soc. Rev.* **2014**, *43*, 7536−7547.

(11) Tsuji, Y.; Yoshizawa, K. Adsorption and Activation of Methane on the (110) Surface of Rutile-type Metal Dioxides. *J. Phys. Chem. C* **2018**, *122*, 15359−15381.

(12) Fung, V.; Tao, F.; Jiang, D.-E. Low-temperature activation of methane on doped single atoms: descriptor and prediction. *Phys. Chem. Chem. Phys.* **2018**, *20*, 22909−22914.

(13) Latimer, A. A.; Kulkarni, A. R.; Aljama, H.; Montoya, J. H.; Yoo, J. S.; Tsai, C.; Abild-Pedersen, F.; Studt, F.; Nørskov, J. K. Understanding trends in C−H bond activation in heterogeneous catalysis. *Nat. Mater.* **2017**, *16*, 225−229.

(14) Ma, X.; Sun, K.; Liu, J.-X.; Li, W.-X.; Cai, X.; Su, H.-Y. Single Ru Sites-Embedded Rutile TiO2 Catalyst for Non-Oxidative Direct Conversion of Methane: A First-Principles Study. *J. Phys. Chem. C* **2019**, *123*, 14391−14397.

(15) Pérez-Ramírez, J.; López, N. Strategies to break linear scaling relationships. *Nat. Catal.* **2019**, *2*, 971−976.

(16) Yuan, K.; Zhong, J.-Q.; Zhou, X.; Xu, L.; Bergman, S. L.; Wu, K.; Xu, G. Q.; Bernasek, S. L.; Li, H. X.; Chen, W. Dynamic oxygen on surface: catalytic intermediate and coking barrier in the modeled CO2 reforming of CH4 on Ni(111). *ACS Catal.* **2016**, *6*, 4330−4339.

(17) Rodriguez, J. A.; Zhang, F.; Liu, Z.; Senanayake, S. D., Methane activation and conversion on well-defined metal-oxide Surfaces:in situstudies with synchrotron-based techniques. In *Catalysis: Volume 31*, The Royal Society of Chemistry: 2019; *31*, 198−215.

(18) Lustemberg, P. G.; Ramírez, P. J.; Liu, Z.; Gutiérrez, R. A.; Grinter, D. G.; Carrasco, J.; Senanayake, S. D.; Rodriguez, J. A.; Ganduglia-Pirovano, M. V. Room-Temperature Activation of Methane and Dry Re-forming with CO2 on Ni-CeO2(111) Surfaces: Effect of Ce3+ Sites and Metal−Support Interactions on C−H Bond Cleavage. *ACS Catal.* **2016**, *6*, 8184−8191.

(19) Liu, Z.; Lustemberg, P.; Gutiérrez, R. A.; Carey, J. J.; Palomino, R. M.; Vorokhta, M.; Grinter, D. C.; Ramírez, P. J.; Matolín, V.;

Nolan, M.; Ganduglia-Pirovano, M. V.; Senanayake, S. D.; Rodriguez, J. A. In Situ Investigation of Methane Dry Reforming on Metal/Ceria(111) Surfaces: Metal−Support Interactions and C−H Bond Activation at Low Temperature. *Angew. Chem., Int. Ed.* **2017**, *56*, 13041−13046.
(20) Lustemberg, P. G.; Palomino, R. M.; Gutierrez, R. A.; Grinter, D. C.; Vorokhta, M.; Liu, Z. Y.; Ramirez, P. J.; Matolin, V.; Ganduglia-Pirovano, M. V.; Senanayake, S. D.; Rodriguez, J. A. Direct Conversion of Methane to Methanol on Ni-Ceria Surfaces: Metal-Support Interactions and Water-Enabled Catalytic Conversion by Site Blocking. *J. Am. Chem. Soc.* **2018**, *140*, 7681−7687.
(21) Besenbacher, F.; Chorkendorff, I.; Clausen, B.; Hammer, B.; Molenbroek, A.; Nørskov, J. K.; Stensgaard, I. Design of a surface alloy catalyst for steam reforming. *Science* **1998**, *279*, 1913−1915.
(22) Rostrupnielsen, J. R.; Hansen, J. H. B. CO2-reforming of methane over transition metals. *J. Catal.* **1993**, *144*, 38−49.
(23) Womes, M.; Cholley, T.; Le Peltier, F.; Morin, S.; Didillon, B.; Szydlowski-Schildknecht, N. Study of the reaction mechanisms between Pt(acac) 2 and alumina surface sites: Application to a new refilling technique for the controlled variation of the particle size of Pt/Al2O3 catalysts. *Appl. Catal. A: Gen.* **2005**, *283*, 9−22.
(24) Ballarini, A.; Basile, F.; Benito, P.; Bersani, I.; Fornasari, G.; De Miguel, S.; Maina, S.; Vilella, J.; Vaccari, A.; Scelza, O. Platinum supported on alkaline and alkaline earth metal-doped alumina as catalysts for dry reforming and partial oxidation of methane. *Appl. Catal. A: Gen.* **2012**, *433-434*, 1−11.
(25) Elsayed, N. H.; Roberts, N. R.; Joseph, B.; Kuhn, J. N. Low temperature dry reforming of methane over Pt−Ni−Mg/ceria−zirconia catalysts. *Appl. Catal. B: Environ.* **2015**, *179*, 213−219.
(26) Zhu, Y.; Chen, K.; Yi, C.; Mitra, S.; Barat, R. Dry reforming of methane over palladium−platinum on carbon nanotube catalyst. *Chem. Eng. Commun.* **2018**, *205*, 888−896.
(27) Damyanova, S.; Pawelec, B.; Arishtirova, K.; Huerta, M. M.; Fierro, J. The effect of CeO2 on the surface and catalytic properties of Pt/CeO2−ZrO2 catalysts for methane dry reforming. *Appl. Catal. B: Environ.* **2009**, *89*, 149−159.
(28) Wu, H.; Pantaleo, G.; La Parola, V.; Venezia, A. M.; Collard, X.; Aprile, C.; Liotta, L. F. Bi-and trimetallic Ni catalysts over Al2O3 and Al2O3-MOx (M= Ce or Mg) oxides for methane dry reforming: Au and Pt additive effects. *Appl. Catal. B: Environ.* **2014**, *156-157*, 350−361.
(29) García-Diéguez, M.; Pieta, I.; Herrera, M.; Larrubia, M.; Alemany, L. Nanostructured Pt-and Ni-based catalysts for CO2-reforming of methane. *J. Catal.* **2010**, *270*, 136−145.
(30) Choudhary, T. V.; Aksoylu, E.; Wayne Goodman, D. Nonoxidative activation of methane. *Catal. Rev.* **2003**, *45*, 151−203.
(31) Schoofs, G. R.; Arumainayagam, C. R.; McMaster, M. C.; Madix, R. J. Dissociative chemisorption of methane on Pt(111). *Surf. Sci.* **1989**, *215*, 1−28.
(32) Marsh, A. L.; Becraft, K. A.; Somorjai, G. A. Methane dissociative adsorption on the Pt (111) surface over the 300− 500 K temperature and 1− 10 Torr pressure ranges. *J. Phys. Chem. B* **2005**, *109*, 13619−13622.
(33) Petersen, M. A.; Jenkins, S. J.; King, D. A. Theory of Methane Dehydrogenation on Pt {110}(1 × 2). Part I: Chemisorption of CHx (x= 0− 3). *J. Phys. Chem. B* **2004**, *108*, 5909−5919.
(34) Nave, S.; Tiwari, A. K.; Jackson, B. Methane dissociation and adsorption on Ni(111), Pt(111), Ni(100), Pt(100), and Pt(110)-(1 × 2): energetic study. *J. Chem. Phys.* **2010**, *132*, No. 054705.
(35) Daelman, N.; Capdevila-Cortada, M.; López, N. Dynamic charge and oxidation state of Pt/CeO2 single-atom catalysts. *Nat. Mater.* **2019**, *18*, 1215−1221.
(36) Brummel, O.; Waidhas, F.; Faisal, F.; Fiala, R.; Vorokhta, M.; Khalakhan, I.; Dubau, M.; Figueroba, A.; Kovács, G.; Aleksandrov, H. A.; Vayssilov, G. N.; Kozlov, S. M.; Neyman, K. M.; Matolín, V.; Libuda, J. Stabilization of Small Platinum Nanoparticles on Pt−CeO2 Thin Film Electrocatalysts During Methanol Oxidation. *J. Phys. Chem. C* **2016**, *120*, 19723−19736.
(37) Bruix, A.; Rodriguez, J. A.; Ramírez, P. J.; Senanayake, S. D.; Evans, J.; Park, J. B.; Stacchiola, D.; Liu, P.; Hrbek, J.; Illas, F. A New Type of Strong Metal−Support Interaction and the Production of H2 through the Transformation of Water on Pt/CeO2(111) and Pt/CeOx/TiO2(110) Catalysts. *J. Am. Chem. Soc.* **2012**, *134*, 8968−8974.
(38) Paffett, M. T.; Gebhard, S. C.; Windham, R. G.; Koel, B. E. Chemisorption of carbon monoxide, hydrogen, and oxygen on ordered tin/platinum (111) surface alloys. *J. Phys. Chem.* **1990**, *94*, 6831−6839.
(39) Pirug, G.; Bonzel, H. P.; Brodén, G. The adsorption of potassium on Pt (111) and its effect on oxygen adsorption. *Surf. Sci.* **1982**, *122*, 1−20.
(40) Pereira-Hernández, X. I.; DeLaRiva, A.; Muravev, V.; Kunwar, D.; Xiong, H.; Sudduth, B.; Engelhard, M.; Kovarik, L.; Hensen, E. J. M.; Wang, Y.; Datye, A. K. Tuning Pt-CeO2 interactions by high-temperature vapor-phase synthesis for improved reducibility of lattice oxygen. *Nat. Commun.* **2019**, *10*, 1358.
(41) Dvořák, F.; Farnesi Camellone, M.; Tovt, A.; Tran, N.-D.; Negreiros, F. R.; Vorokhta, M.; Skála, T.; Matolínová, I.; Mysliveček, J.; Matolín, V.; Fabris, S. Creating single-atom Pt-ceria catalysts by surface step decoration. *Nat. Commun.* **2016**, *7*, No. 10801.
(42) Lustemberg, P. G.; Zhang, F.; Gutiérrez, R. A.; Ramírez, P. J.; Senanayake, S. D.; Rodriguez, J. A.; Ganduglia-Pirovano, M. V. Breaking Simple Scaling Relations through Metal−Oxide Interactions: Understanding Room-Temperature Activation of Methane on M/CeO2 (M = Pt, Ni, or Co) Interfaces. *J. Phys. Chem. Lett.* **2020**, *11*, 9131−9137.
(43) Dablemont, C.; Lang, P.; Mangeney, C.; Piquemal, J.-Y.; Petkov, V.; Herbst, F.; Viau, G. FTIR and XPS Study of Pt Nanoparticle Functionalization and Interaction with Alumina. *Langmuir* **2008**, *24*, 5832−5841.
(44) Fu, X.; Wang, Y.; Wu, N.; Gui, L.; Tang, Y. Surface Modification of Small Platinum Nanoclusters with Alkylamine and Alkylthiol: An XPS Study on the Influence of Organic Ligands on the Pt 4f Binding Energies of Small Platinum Nanoclusters. *J. Colloid Interface Sci.* **2001**, *243*, 326−330.
(45) Mullins, D. R. The surface chemistry of cerium oxide. *Surf. Sci. Rep.* **2015**, *70*, 42−85.
(46) Nishiyama, N.; Yamazaki, S. Effect of mixed valence states of platinum ion dopants on the photocatalytic activity of titanium dioxide under visible light irradiation. *ACS Omega* **2017**, *2*, 9033−9039.
(47) Guda, A. A.; Bugaev, A. L.; Kopelent, R.; Braglia, L.; Soldatov, A. V.; Nachtegaal, M.; Safonova, O. V.; Smolentsev, G. Fluorescence-detected XAS with sub-second time resolution reveals new details about the redox activity of Pt/CeO2 catalyst. *J. Synchrotron Radiat.* **2018**, *25*, 989−997.
(48) Setthapun, W.; Williams, W. D.; Kim, S. M.; Feng, H.; Elam, J. W.; Rabuffetti, F. A.; Poeppelmeier, K. R.; Stair, P. C.; Stach, E. A.; Ribeiro, F. H. Genesis and evolution of surface species during Pt atomic layer deposition on oxide supports characterized by in situ XAFS analysis and water− gas shift reaction. *J. Phys. Chem. C* **2010**, *114*, 9758−9771.
(49) Uemura, Y.; Inada, Y.; Bando, K. K.; Sasaki, T.; Kamiuchi, N.; Eguchi, K.; Yagishita, A.; Nomura, M.; Tada, M.; Iwasawa, Y. In situ time-resolved XAFS study on the structural transformation and phase separation of Pt3Sn and PtSn alloy nanoparticles on carbon in the oxidation process. *Phys. Chem. Chem. Phys.* **2011**, *13*, 15833−15844.
(50) Akri, M.; Zhao, S.; Li, X.; Zang, K.; Lee, A. F.; Isaacs, M. A.; Xi, W.; Gangarajula, Y.; Luo, J.; Ren, Y. Atomically dispersed nickel as coke-resistant active sites for methane dry reforming. *Nat. Commun.* **2019**, *10*, 1−10.
(51) Tang, Y.; Wei, Y.; Wang, Z.; Zhang, S.; Li, Y.; Nguyen, L.; Li, Y.; Zhou, Y.; Shen, W.; Tao, F. F.; Hu, P. Synergy of Single-Atom Ni1 and Ru1 Sites on CeO2 for Dry Reforming of CH4. *J. Am. Chem. Soc.* **2019**, *141*, 7283−7293.

https://dx.doi.org/10.1021/acscatal.0c04694
ACS Catal. 2021, 11, 1613−1623

(52) Turap, Y.; Wang, I.; Fu, T.; Wu, Y.; Wang, Y.; Wang, W. Co−Ni alloy supported on CeO2 as a bimetallic catalyst for dry reforming of methane. *Int. J. Hydrogen Energy* **2020**, *45*, 6538−6548.
(53) Rameshan, C.; Li, H.; Anic, K.; Roiaz, M.; Pramhaas, V.; Rameshan, R.; Blume, R.; Hävecker, M.; Knudsen, J.; Knop-Gericke, A. In situ NAP-XPS spectroscopy during methane dry reforming on ZrO2/Pt(1 1 1) inverse model catalyst. *J. Phys.: Condens. Matter* **2018**, *30*, No. 264007.
(54) Zhang, F.; Liu, Z.; Chen, X.; Rui, N.; Betancourt, L. E.; Lin, L.; Xu, W.; Sun, C.-j.; Abeykoon, A. M. M.; Rodriguez, J. A.; Teržan, J.; Lorber, K.; Djinović, P.; Senanayake, S. D. Effects of Zr Doping into Ceria for the Dry Reforming of Methane over Ni/CeZrO2 Catalysts: In Situ Studies with XRD, XAFS, and AP-XPS. *ACS Catal.* **2020**, *10*, 3274−3284.
(55) Wolfbeisser, A.; Sophiphun, O.; Bernardi, J.; Wittayakun, J.; Föttinger, K.; Rupprechter, G. Methane dry reforming over ceria-zirconia supported Ni catalysts. *Catal. Today* **2016**, *277*, 234−245.
(56) Weaver, J. F.; Carlsson, A. F.; Madix, R. J. The adsorption and reaction of low molecular weight alkanes on metallic single crystal surfaces. *Surf. Sci. Rep.* **2003**, *50*, 107−199.
(57) Freund, H.-J.; Roberts, M. W. Surface chemistry of carbon dioxide. *Surf. Sci. Rep.* **1996**, *25*, 225−273.
(58) Dai, C.; Zhang, S.; Zhang, A.; Song, C.; Shi, C.; Guo, X. Hollow zeolite encapsulated Ni−Pt bimetals for sintering and coking resistant dry reforming of methane. *J. Mater. Chem. A* **2015**, *3*, 16461−16468.
(59) Chen, L.; Huang, Q.; Wang, Y.; Xiao, H.; Liu, W.; Zhang, D.; Yang, T. Tailoring performance of Co−Pt/MgO−Al2O3 bimetallic aerogel catalyst for methane oxidative carbon dioxide reforming: Effect of Pt/Co ratio. *Int. J. Hydrogen Energy* **2019**, *44*, 19878−19889.
(60) Parkinson, G. S. Unravelling single atom catalysis: The surface science approach. *Chin. J. Catal.* **2017**, *38*, 1454−1459.
(61) Ravel, B.; Newville, M. ATHENA, ARTEMIS, HEPHAESTUS: data analysis for X-ray absorption spectroscopy using IFEFFIT. *J. Synchrotron Radiat.* **2005**, *12*, 537−541.
(62) Chupas, P. J.; Chapman, K. W.; Kurtz, C.; Hanson, J. C.; Lee, P. L.; Grey, C. P. A versatile sample-environment cell for non-ambient X-ray scattering experiments. *J. Appl. Crystallogr.* **2008**, *41*, 822−824.
(63) Toby, B. H.; Von Dreele, R. B. GSAS-II: the genesis of a modern open-source all purpose crystallography software package. *J. Appl. Crystallogr.* **2013**, *46*, 544−549.
(64) Resasco, J.; DeRita, L.; Dai, S.; Chada, J. P.; Xu, M.; Yan, X.; Finzel, J.; Hanukovich, S.; Hoffman, A. S.; Graham, G. W.; Bare, S. R.; Pan, X.; Christopher, P. Uniformity Is Key in Defining Structure−Function Relationships for Atomically Dispersed Metal Catalysts: The Case of Pt/CeO2. *J. Am. Chem. Soc.* **2020**, *142*, 169−184.

https://dx.doi.org/10.1021/acscatal.0c04694
ACS Catal. 2021, 11, 1613−1623